

# Current-Driven Mode Free Reversed Field Pinch Plasma with Resistive Shell

Yoshiki MAEJIMA and Hisao ASHIDA

The stability of reversed field pinch(RFP) plasma configurations is studied by comparing the linear growth-rate of MHD modes. The experimental RFP are operating just on the boarder of the stability boundary of MHD modes near the plasma center, which sustain the RFP equilibrium configuration as “Dynamo action”. In the experimental configuration sustained by the dynamo-mode, the shell proximity of 1.15 is a very sever condition and the  $\beta_p$  is limited to low value of 0.12. In the case of the current-driven mode free configuration, twice higher  $\beta_p$  is possible with lose fitting shell of 1.6. The  $\beta_p$  scaling deriving from turbulence driven by the resistive g-mode balanced with ohmic heating power will be discussed

## §1 Introduction

The experimental reversed field pinch(RFP) plasmas are operating just on the boarder of the stability boundary of MHD modes near the plasma center, which sustain the RFP equilibrium configuration as “dynamo action”, the MHD dynamo model. The loop voltage of experimental RFP increases with poor shell proximity as the linear growth-rate of dynamo modes increase quickly. MHD equilibrium and stability of RFP configurations are studied using a resistive MHD

stability code<sup>1)</sup> to estimate the maximum  $\beta_p$  and the farthest shell position. Dynamo-mode free RFP configurations and  $\beta_p$  scaling will be discussed.

## §2 Experimental RFP equilibrium configuration

Equilibrium configurations of RFP plasmas are characterized by pinch parameter  $\theta(=B_p(a)/B_{t\_av})$  and reversal parameter  $F(=B_t(a)/B_{t\_av})$ , where  $B_p, B_t$  and  $B_{t\_av}$  are poloidal, toroidal and average toroidal

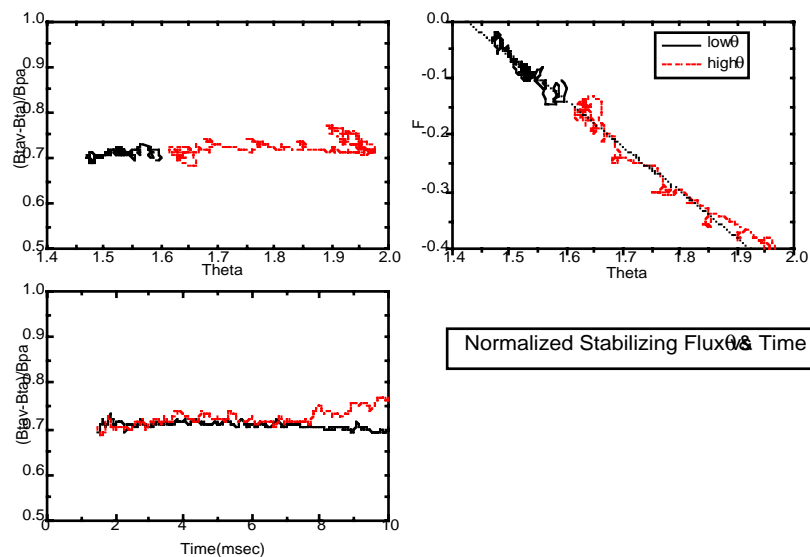
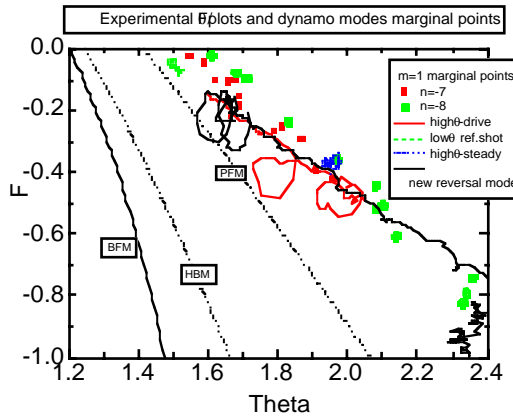


Fig.1 Normalized stabilizing flux,  $(1-F)/\theta$  vs  $\theta$  time for low and high  $\theta$  discharges.

KEY WORDS : Reversed field pinch, dynamo-mode, resistive shell, resistive g-mode, poloidal



**Fig.2** Experimental  $F/\theta$  plots with marginal stability points of dynamo-mode,  $m=1/n=-7$  &  $-8$ .

magnetic field respectively and  $a$  is plasma minor radius. As shown in **Fig.1** experimental  $F/q$  points have a unique feature such that they follow a straight line of  $F=1-C*\theta$ , where  $C=0.7\sim 0.75$  in TPE-1RM20<sup>2)</sup> as observed in many other RFP devices. TPE-Z toroidal z-pinch plasma, where no toroidal field coil exists, shows a similar result such as the operational  $\theta$  is limited of around 1.5 where  $F=0$ . The constant slope,  $C=(1-F)/\theta=(Bt_{av}-Bt(a))/Bp(a)$ , means that the stabilizing toroidal flux (i.e. paramagnetic component) inside the plasma is proportional to the plasma current in experimental RFP plasmas. The normalized stabilizing toroidal flux  $C$  is independent of the plasma current and the pinch ratio  $\theta$  in TPE-1RM20. The study of the equilibrium configurations by the resistive MHD stability code suggests that the experimental  $F/\theta$  points follow the dynamo-mode marginal stability points as shown in **Fig.2**. Rothenbluth reported the similar result on the stabilizing toroidal flux required for a stable pinch plasma with sharp boundary<sup>3)</sup>. RFP plasmas in

experiments are operating just on the stability boundary of tearing modes near the plasma center, which sustain the RFP configuration as “dynamo action”.

### §3 Loop Voltages of RFP with resistive shell

The loop voltage of RFP increases with poor shell proximity as the linear growth-rate of dynamo modes increase quickly. Fully nonlinear calculations give the loop voltage of steady state RFP configurations sustained by the dynamo modes<sup>4)</sup>. To estimate the loop voltage dependence on the shell proximity by a linear calculation, the poloidal electric fields created by the dynamo mode and of the equilibrium resistive component is balanced and the toroidal electric field at the plasma center by the mode is defined as the loop voltage increase.

**Fig.3** shows the toroidal electric field,  $E_z(=E_{z_{mode}}+E_{z_{\eta j0}})/E_{z_{\eta j0}}$ , dependence on the perfect shell position and resistive shell time constant. The loop voltage increase is clearly seen. An equilibrium configuration is created by the  $\alpha$ -model<sup>5)</sup>,  $\theta/F=1.9/-0.38(\theta_0/\alpha=1.9/2.3)$  with  $\beta p=0.15$ . The Magnetic Reynolds number of  $10^5$  is used in the calculation. A single  $m=1/n=-7$  mode selected is the non-resonant dynamo mode. When the perfect shell moves away from the plasma surface, the  $E_{\theta_{mode}}$  quickly decreases its amplitude and moves the peak position out, while  $E_{z_{mode}}$  is not changed much. The  $\langle b_r x v_z \rangle$  term of the  $E_{\theta_{mode}}$  decreases the amplitude and the  $\langle b_z x v_r \rangle$  term, which has opposite sign, increases. Here  $b_r, b_z, v_r$  and  $v_z$  are mode components. The main reason is that the  $b_r$  decrease and the  $v_r$  increase with moving the boundary condition out. As

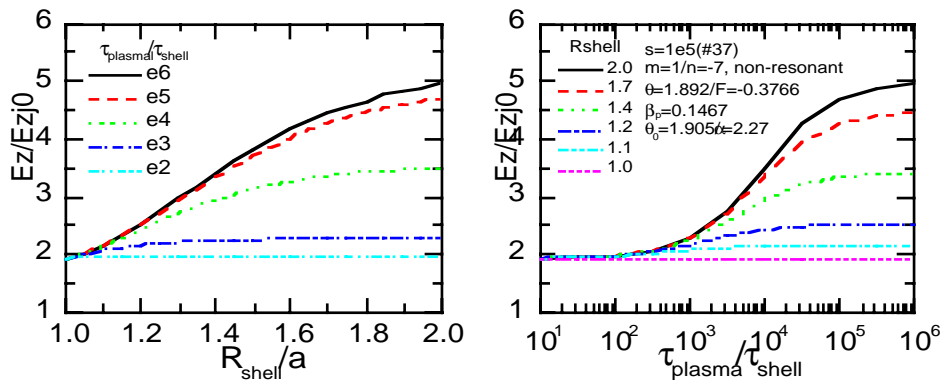


**Fig.3** Normalized toroidal electric field,  $E_z(=E_{z_{mode}}+E_{z_{\eta j0}})/E_{z_{\eta j0}}$ , dependence on perfect shell position and resistive shell time constant.

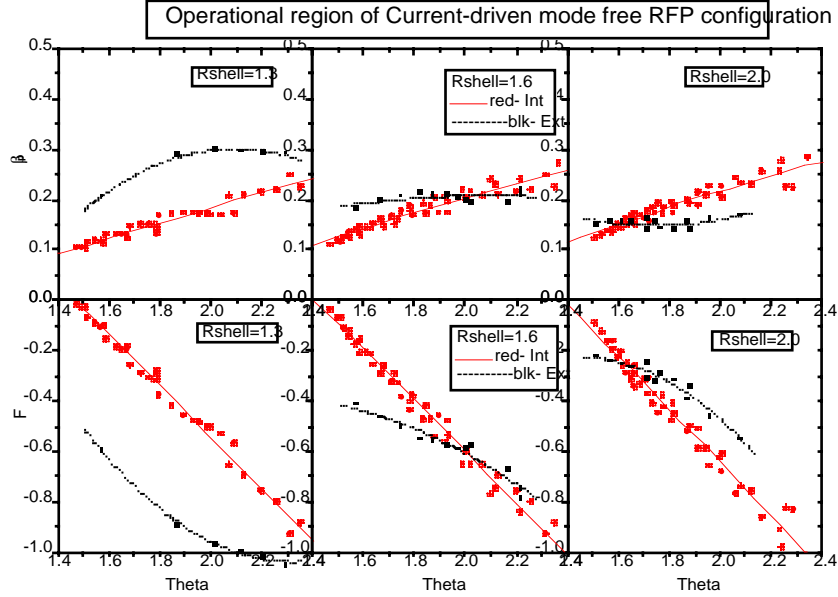


**Fig.4** Operational regions of current-driven mode free RFP configuration with  $\beta_p$  on perfect shell position. Regions are stable against both  $m=1$  internal mode (red) and external mode (black).

the result the dynamo-mode efficiency on creating the poloidal electric field drops with the poor shell condition and the larger toroidal electric field results required. In the case of the nonlinear situation as the resistive shell decreases its stabilizing effect to quasi steady state MHD mode, the effective resistive shell time results decrease. In experimental RFPs much larger loop voltages are required. The helicity leakage by the edge plasma turbulence may be responsible.

**§4 Current-driven mode free RFP configuration**

RFP configurations having a resistive shell without both the  $m=1$  internal and the external ideal MHD and tearing mode are investigated. Equilibrium configurations are constructed by using  $\alpha$ - $\theta_0$  model for  $\mu$  ( $=J/B$ ) profile, where  $\mu=2*\theta_0(1-(r/a)^\alpha)$ . Plasma pressure is inflated by Suydam parameter  $C_{suydam}(r) = -4\pi r^{1/2} / (rB_z^2)(q/q')^2$ , keeping the  $q$ -profile same to identify modes between ideal MHD, tearing and resistive  $g$ -mode, with a window function to decrease pressure gradient near the plasma edge. The stability of RFP plasma configurations are subject to the  $m=1$  internal and external ideal MHD and tearing modes as global modes (In RFP the internal and the external is defined relative to the  $B_t$  reversal surface). The  $m=0$  tearing mode also exists in poor shell proximity condition, but has generally low growth-rate and is not

global like  $m=1$  mode. Stability is compared by the linear growth-rate with conditions of  $S$  (Magnetic Reynolds number)  $=10^4$ ,  $r_{mesh}=91$  and aspect ratio of 3.9. The operational regions of current-driven mode free RFP configuration are given between the internal and the external mode stability boundaries as shown in Fig.3. Typical results are <sup>6)</sup>: (1) Current-driven mode free RFP configurations are possible with a lose-fitting perfect conducting shell. Maximum perfect shell positions is  $r_{shell}/a$  of 2 with  $\beta_p$  of 0.14 against both  $m=1$  internal and external modes, while maximum  $\beta_p$  of 0.3 is possible if  $r_{shell}/a$  is located closer at 1.2 as shown in Fig.4.

(2) In case of OH sustained experimental RFP configuration described before,  $r_{shell}/a$  of 1.15 is the

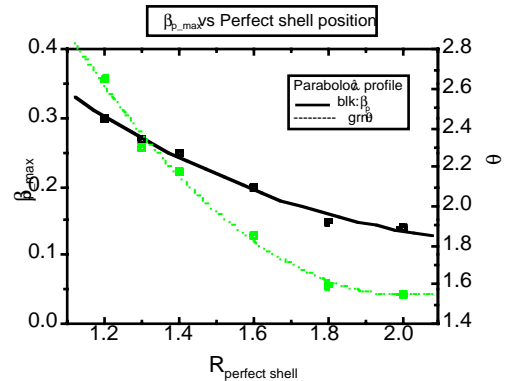


**Fig.5** Maximum  $\beta_p$  vs perfect shell position for current-driven mode free configuration.

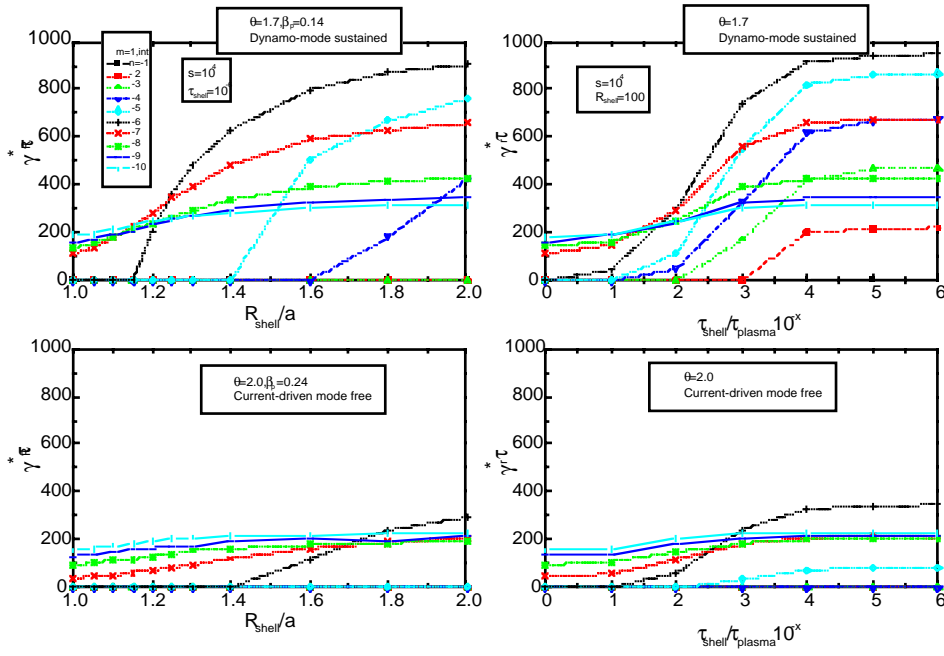


Fig.6 Linear growth-rates vs perfect shell position and resistive shell time constant

limit against the resistive shell mode as shown in Fig.5 and the  $\beta_p$  is lowered around 0.12.

(3) Resistive wall with resistive shell time constant of  $<10^{-3}$  has almost no effect as the stabilizing shell to MHD modes, which is also shown in Fig.6.

§5 S scaling of linear growth-rate

Dependency of modes on Magnetic Reynolds number in the code is briefly checked. On dynamo-mode: The tearing mode without plasma pressure scales as  $S^{2/5}$  when  $S < 10^6$ . While the pressure is inflated, the mode scales as  $S^{2/3}$  like the resistive g-mode. When the mode becomes non-singular, the mode scales  $S^{1.0}$  as ideal MHD mode. The linear growth-rate has maximum at the mode's singular moves just the plasma center off.

On resistive g-mode: The resistive g-mode scale as  $S^{2/3}$  when  $S < 10^6$ . If the pressure is inflated much higher than Suydam condition, i.e. Suydam unstable, the mode scales as  $S^{1.0}$  like ideal MHD mode. The  $m=0$  mode has lower growth-rate than the  $m=1$  mode. When  $S$  is larger than  $10^6$ , any mode scales as  $S^{1.0}$  in this code.

§6  $\beta_p$  scaling by resistive g-mode

Current-driven mode free RFP is possible, but there

still remain the resistive g-modes in RFP plasma. The linear growth-rate of resistive g-modes is studied to get a  $\beta_p$  scaling on  $S$ . Result shows that the linear growth-rate of g-mode is proportional to  $\beta_p$  as  $\gamma(\tau_R^{-1}) = 4.3 * \beta_p * S^{2/3}$ , while the growth-rate increases more rapidly in case of the higher  $\beta_p$  than the Suydam limit. In Fig.7 the linear growth-rate of  $m=1/n=-32$  g-mode vs.  $\beta_p$  is shown. A simple model that the loss rate by the several times of the linear growth-rate above is balanced with joule input power derives a scaling of  $\beta_p \sim a^{-2/5} * ip^{-4/5}$  for g-mode. If heating power is higher enough than the loss rate,  $\beta_p$  is limited by the Suydam condition.

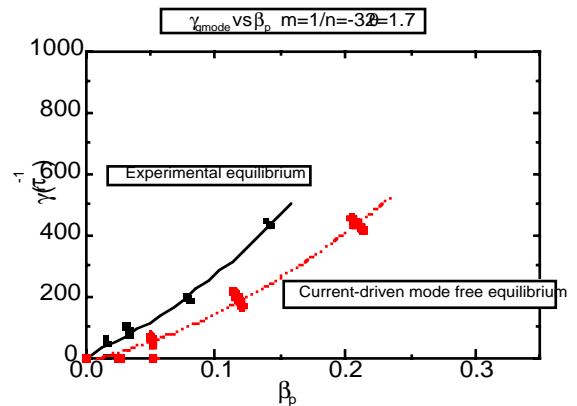


Fig.7 Linear growth-rates of  $m=1/n=-32$  resistive g-mode vs  $\beta_p$

## §7 Summary

The stabilities of RFP plasma configurations are studied by comparing the linear growth-rate of MHD modes. In the experimental configuration sustained by the dynamo-mode, the shell proximity of 1.15 is a very sever condition and the  $\beta_p$  is limited to low value. In the case of the current-driven mode free configuration, higher  $\beta_p$  is possible with lose fitting shell of 1.6. The  $\beta_p$  scaling deriving from turbulence driven by the resistive g-mode balanced with ohmic heating power implies decreasing  $\beta_p$  in larger RFP devices. Suppression of turbulence will be necessary.

## References

- 1) H.Ashida, et al.: Bul. Electrotech. Lab. **49**(10), (1985)794.
- 2) Y.Maejima, et al.: 3a-YM-6, *51th Annual meeting*, PSJ(1996).
- 3) M.N.Rothenbluth: "Stability of the Pinch." Report LA-2030(1956).
- 4) D.D.Schnack,S.Ortolani: Nuclear Fusion **30**(2),(1990)277.
- 5) V.Antoni,et al: Nuclear Fusion **26**(12),(1986)1711.
- 6) Y.Maejima,H.Ashida: pThpP3.29, *APS\_DPP97*(1997).  
(Accepted February 15, 1999)

## Authors



**Yoshiki MAEJIMA**  
Energy Fundamentals Div. Plasma theory lab.  
E-mail: maejima@etl.go.jp  
Study on exporimental physics of fusion plasma  
and plasma diagnostics.



**Hisao ASHIDA**  
Energy Fundamentals Div. Plasma theory lab.  
E-mail: ashida@etl.go.jp  
Study on theoretical physics of MHD equilibrium  
and stability in fusion plasma.